High-Voltage Cable Modeling Using *DEFINE_CABLE: Optimization and Validation for Automotive Crash Applications

Maximilian Beck[1], Raphael Heiniger[2]

[1]BMW Group
[2]Ansys, part of Synopsys

1 Abstract

The increasing complexity of high-voltage cable systems in automotive safety applications demands advanced modeling techniques to accurately predict their mechanical behavior under various load conditions. This study investigates the potential of the recently introduced **`*DEFINE_CABLE`** keyword as a novel approach to cable modeling. By focusing on axial tension, three-point bending, and radial compression load cases, the research aims to assess the capabilities and limitations of this method compared to existing techniques. The motivation lies in improving simulation accuracy and efficiency, particularly for complex load scenarios, while addressing the challenges posed by non-linear material behavior, mesh dependencies and numerical stability in high-voltage cable systems.

2 Introduction

Crush of high-voltage (HV) cables in automotive crash as show in Fig. 1 can precipitate short-circuit, arcing, and thermal events that endanger occupants and first responders. Hidden internal damage and short-duration squeezing in physical tests are difficult to detect, motivating an approach for early, virtual risk assessment and design optimization (routing, shielding, HV shut-off timing). We employ the keyword **`*DEFINE_CABLE`** present in Ansys LS-DYNA R16 to generate analyzable solid element cables with beam-based cable chains as backbone. We investigate material models and parameters, mesh size, element formulation while balancing accuracy, mass scaling and runtime within industrial automotive crash models. The objective is a validated, mechanically driven indicator for short-circuit risk derived from simulation outputs.

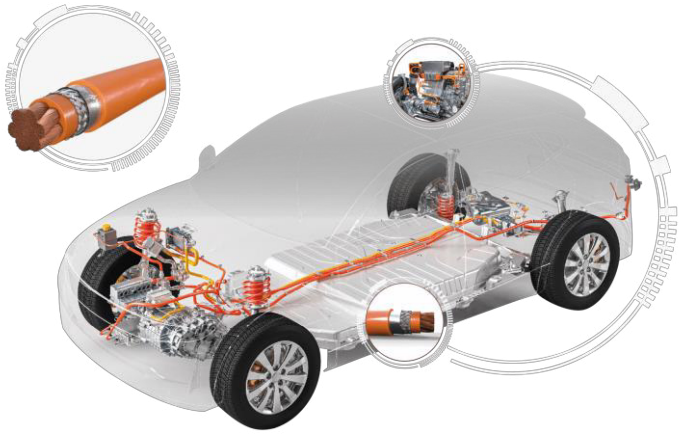

Fig. 1: High voltage cables in electric vehicle powertrains [1]

3 Modeling strategy

In this section we outline the four modeling strategies which are evaluated to represent the mechanical response of high-voltage cables under crash-induced deformation. Further we describe the modeling approach using **`*DEFINE_CABLE`** which is based on the approach described in 3.1.3 1D & (2D) & 3D.

3.1 State-of-the-art modeling strategies

The Fig. 2 shows the evaluated models which are described in detail in the next sections.

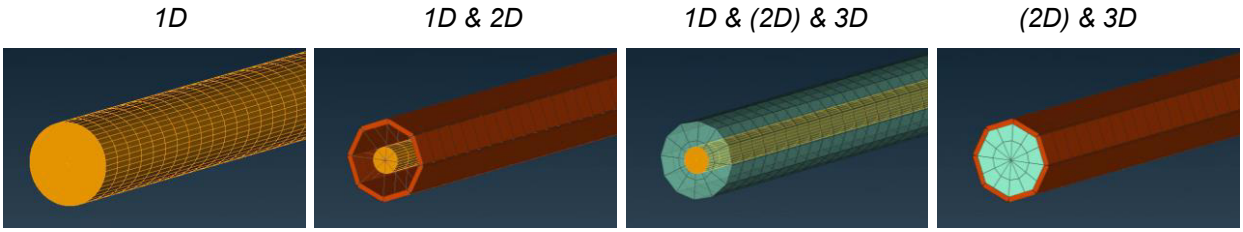

Fig. 2: Different modeling strategies for cables

3.1.1 1D

This approach employs beam or truss elements along the cable's longitudinal axis. It captures axial tension/compression and bending or torsion about the axis. The method is computationally efficient but cannot reproduce radial crushing or volumetric effects. Material calibration complexity is low.

3.1.2 1D & 2D

The cable core is modeled with beam or truss elements, while the sheath is represented by shell elements. Additional radial beams or contact aids improve local interactions. This configuration enhances contact fidelity and allows limited radial crushing in discrete sections. However, it suffers from stability issues under severe deformation and lacks full volumetric response. Calibration complexity is moderate.

3.1.3 1D & (2D) & 3D

This hybrid strategy combines a beam backbone with optional shell layers and solid elements to represent volumetric behavior. It captures axial, bending, and torsional stiffness as well as transversal crushing and shear deformation. The approach provides a good balance between accuracy and computational cost. Calibration complexity is high.

3.1.4 (2D) & 3D

This method uses solid elements, optionally combined with shell layers, to model the cable in full three-dimensional detail. It offers the most accurate representation of volumetric crushing and shear but is computationally expensive.

3.2 1D & 3D modeling approach with `*DEFINE_CABLE`

One adopts method 1D & 3D in 3.1.3 to use a beam centerline for axial and partially bending behavior and solid sections to capture transversal crushing, shear and bending as well. This approach is compatible with **`*DEFINE_CABLE`** and there for one can leverage **`*DATABASE_CABLE`** outputs for risk metrics. In this section we point out the core features of **`*DEFINE_CABLE`** keyword and dive into the material models used for the beams and the solids.

*3.2.1 *DEFINE_CABLE keyword*

`*DEFINE_CABLE` automates the creation of cable assemblies from an existing beam representation by adding solid and optional shell layers (see Fig. 3). It links cross-sectional data to beam elements and generates connectivity for combined 1D & 3D modelling using **`*DEFINE_CABLE_CONNECTIVITY`**. This approach enables efficient representation of axial, bending, and crushing behavior while maintaining compatibility with standard crash models.

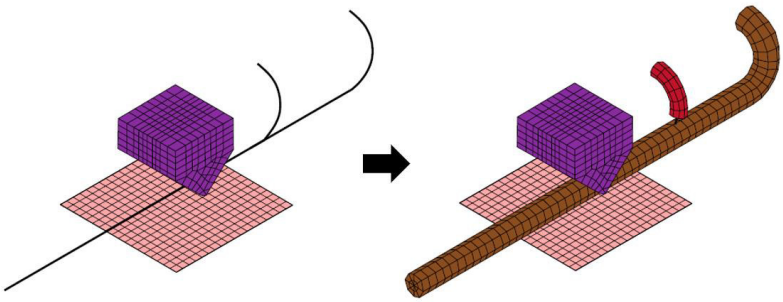

*Fig. 3: Solid generation by ***DEFINE_CABLE** [3]*

***DATABASE_CABLE** provides dedicated output for cable-specific metrics, including:

- Time series of maximum radial stress and force along each beam of the cable (see Fig. 4, left)
- Cross-sectional area evolution
- Time and location of maximum compression
- Summary data per cable and for the entire model (see Fig. 4, right)

These time series are binary output to binout/cable and a summary is written as ASCII file to the result directory. At the time no postprocessor supports the cable binary results.


```
PART-WISE DATA:

 Beam part=   3000002, sampling frequency=        1 cycles
 maxstress=    0.1578E+03, time=    0.1427E-01, element=       3000502
 minarea  =    0.8386E+02, time=    0.1427E-01, element=       3000501
 maxforce =    0.4122E+05, time=    0.1427E-01, element=       3000501

DATA FOR ALL PARTS:

 maxstress=    0.1578E+03, time=    0.1427E-01, element=       3000502, part=       3000002
 minarea  =    0.8386E+02, time=    0.1427E-01, element=       3000501, part=       3000002
 maxforce =    0.4122E+05, time=    0.1427E-01, element=       3000501, part=       3000002
```

Fig. 4: Maximum radial stress along cable beams for specific time extracted from binout with a Python script (left), Summary data as ASCII file (right)

3.2.2 Beam material modeling

Two beam material formulations are considered for representing the axial, bending and torsional behavior of high-voltage cables:

- ***MAT_MOMENT_CURVATURE_BEAM**
  This formulation provides axial stiffness on tension and compression as well as bending and torsional stiffness, enabling a realistic representation of cable kinematics under combined loading. It is mesh-independent with respect to strain, curvature, and twist rate however it uses a force, moment and torque resultant-based approach. This leads to a dependency on the cable diameter, meaning that for each cable diameter required in the model the material model parameters vary.

- ***MAT_CABLE_DISCRETE_BEAM**
  This candidate model is strain and stress based making it mesh- and diameter-independent. However, it lacks bending, compression and torsional stiffness.

The present investigation employs ***MAT_MOMENT_CURVATURE_BEAM** due to its ability to capture essential stiffness contributions however the introduced bending stiffness must be balanced with the bending stiffness introduced by the solid elements to avoid overestimating the total bending stiffness of the cable. Another drawback is the diameter dependency increasing the number of material cards required when multiple diameters are present in a model. Therefore, ***MAT_CABLE_DISCRETE_BEAM** shows potential for future work, as extensions to include torsion and compression stiffness together with the mesh- and diameter independence could significantly improve usability.

3.2.3 Solid material modeling

To represent the complex plastic, rubber, and metallic constituents of the high-voltage cable in a simplified yet realistic way, homogenized solid material models were evaluated and compared for their suitability.

- **`*MAT_PIECEWISE_LINEAR_PLASTICITY`**
  This is an elastic-plastic material model with an arbitrary stress–strain curve and strain-rate dependency. It is relatively simple, requiring only a few calibration parameters such as Young's modulus, tangent modulus, and yield stress. It is well-suited for ductile metals or plastics where bi-linear plasticity is a reasonable assumption.

- **`*MAT_CRUSHABLE_FOAM`**
  This model is commonly applied for plastics, foams, and homogenized materials. It can represent nonlinear compressive behavior with tension cutoff and allows for tuning many parameters, such as stiffness, yield surface, and damping. The model supports rate dependence and is therefore suitable for complex heterogeneous materials that need an effective continuum representation.

- **`*MAT_MODIFIED_HONEYCOMB`**
  This model is often used for cellular or honeycomb-like materials and includes advanced features to capture anisotropic behavior and complex crush responses.

Early attempts to calibrate the radial response using **`*MAT_PIECEWISE_LINEAR_PLASTICITY`** were unsuccessful. The very low initial radial stiffness of the cables required unrealistically low yield parameters, leading to non-physical behavior, while constraining these parameters prevented matching experimental curves which will be described later. Consequently, this approach was abandoned and **`*MAT_CRUSHABLE_FOAM`** was adopted in this work. **`*MAT_MODIFIED_HONEYCOMB`** is not further investigated.

4 Physical testing

Three quasi-static tests were performed to characterize cable mechanics and support model calibration: Axial tension to determine axial stiffness, three-point bending to assess bending flexibility, and radial compression with short-circuit detection under 800 VDC. For radial compression, indenter radius R was varied (R = 50 mm, R = 2 mm and R << 1mm) to capture global and local crushing effects. The tests provided force–displacement curves and identified deformation and force thresholds for electrical short-circuit.

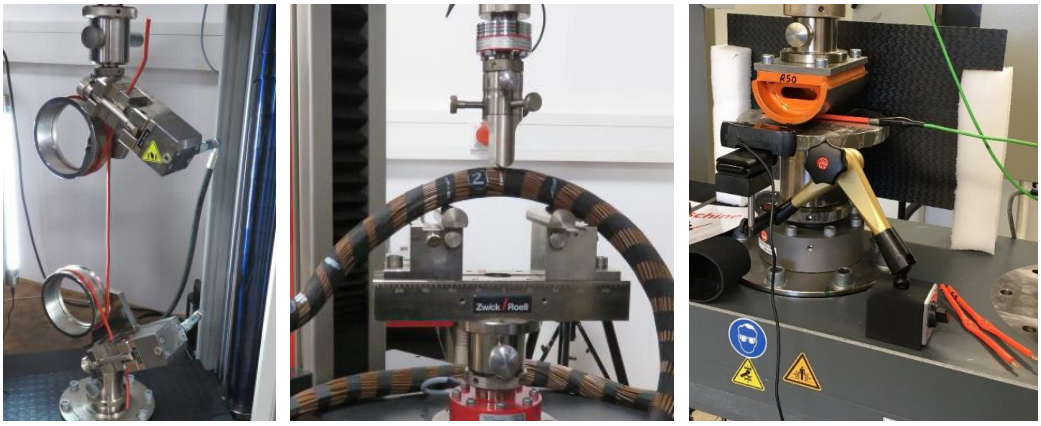

Fig. 5: Physical test setups for axial tension (left), 3-point bending (center) and radial compression with short-circuit detection (right)

5 Calibration and Validation

Material calibration was performed separately for beam and solid components using physical tests. An iterative design of experiments (DOE) approach was used to reduce the parameter space of the optimization. Calibration focuses on matching force-displacement curves and stress-strain behavior. Validation involved comparing simulation results with physical test data across multiple load cases. The workflow from physical tests to the validated models is visualized in Fig. 6.

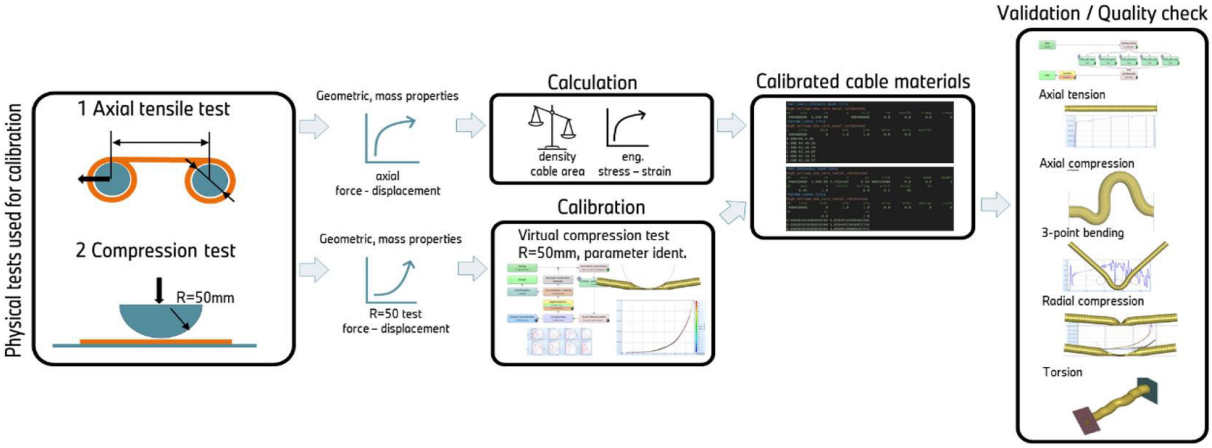

Fig. 6: Overview on workflow from test to the calibration and validation

5.1 Calibration

This chapter outlines the DOE-based parameter studies and subsequent optimization steps used to develop an accurate and efficient cable model.

5.1.1 DOE Studies

Some parameters given by the chosen material models could initially be stated as fixed by taking reasonable assumptions e.g. for the Young's Modulus or other constants. This drastically reduced the variable parameters to a small amount of less than 10. Due to the non-linear stiffness in radial compression observed by physical tests the stress-strain curve for the material model of the solid elements has been identified as the most sensitive parameter. To keep the count of variables as small as possible, instead of a fully variable curve function a parametrized spline with 4 control points and according constraints was introduced to the optimiazation (see Fig. 7).

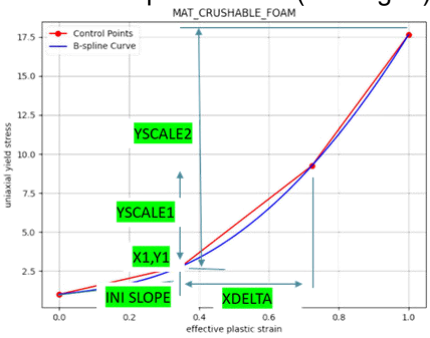

Fig. 7: Parametrized stress-strain curve (4 point spline)

Geometrical parameters, such as the mesh size, are constrained by a fixed time step to be maintained throughout full-vehicle simulations. In pursuit of developing a cable model that robustly matches observed behavior at a reasonable computational cost, the minimum element size was set to 2.5 mm to provide adequate deformation resolution when paired with a sharp-edged indenter of radius R = 2 mm. As the element size decreases, the total element count must be considered in both longitudinal and radial directions to avoid element distortion and poor aspect ratios. Although the large indenter yields a reproducible force–displacement response across mesh sizes, the small indenter is more sensitive to larger element lengths. Conversely, smaller elements increase mass scaling requirements to preserve the time step, thereby extending the simulation runtime by approximately 10%. Consequently, a 5 mm mesh with two layers in the radial direction was selected as the best compromise (see Fig. 8).

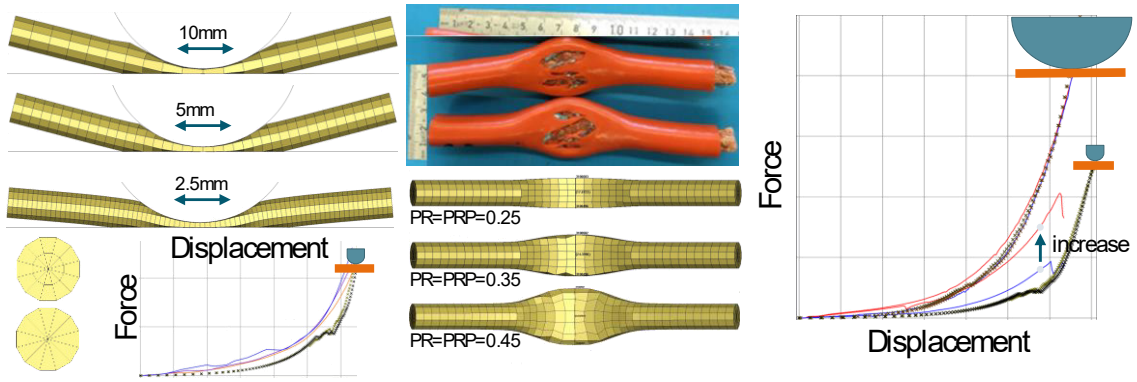

Fig. 8: DOE studies for mesh size (left), Poisson's ration (center) and element formulation (right)

Since deformations occur almost exclusively in the plastic range, the assumption was made to equate the elastic and plastic Poisson's ratios. In the absence of experimental data, a best-practice approach was adopted to approximate a picture like that observed in the post-test photographs. The radial stiffness showed little influence in this context, as expected, because the lateral deformation occurs freely and without constraint. Finally, a Poisson's ratio of 0.45 for PR and PRP was set.
Element formulation was also investigated. The standard crash-simulation convention using under-integrated elements (ELFORM=1) led to an artificially increase in the response with the R = 2 mm indenter by approximately a factor of two. To overcome this fully integrated elements with ELFORM=-1 was chosen as a preferable option.

5.1.2 Final optimization

The optimization for the present cable is carried out in two independent steps. In the first step, the parameters required for the beam material model **`*MAT_MOMENT_CURVATURE_BEAM`** are identified.

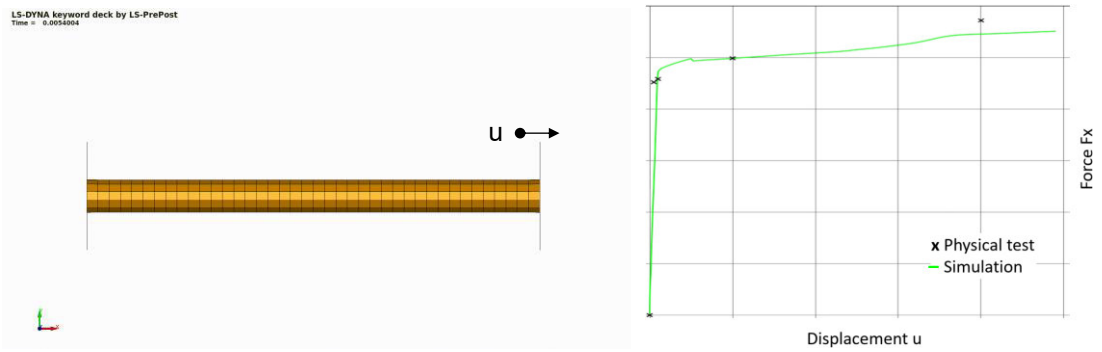

Fig. 9: Radial compression load case (R=2mm) model (left) and physical (black) and the simulated (green) test results (right)

Specifically, the axial force–strain, moment–curvature, and torque–twist rate relationships must be defined, along with the Young's modulus. The axial force–strain curve is constructed by directly using the measured axial force F_x from the tensile test and computing the corresponding Cauchy strain ε_{xx} from the axial displacement u and the specimen length l according to $\varepsilon_{xx} = \frac{u}{l}$. The moment M – curvature κ relationship is derived from three-point bending tests, where the vertical displacement (z-direction) at the mid-span and the applied force in the z-direction F_z are recorded. The bending moment M is calculated from the measured F_z and the span length l_s using $M = \frac{F_z l_s}{4}$. Assuming small deflections and linear geometry the curvature κ is determined from the mid-span deflection δ according to $\kappa = \frac{12\,\delta}{{l_s}^2}$. However, as the introduced bending stiffness of the solid elements turns out to be sufficient the moments are scaled down to a minimum. Some amount of bending stiffness is still required to prevent wrinkling (see Fig. 10).

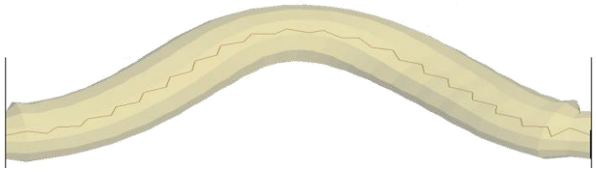

Fig. 10: Beam wrinkling under compression with ****MAT_MOMENT_CURVATURE_BEAM***

Since no experimental data is available for the torque–twist rate relationship, it is estimated based on the theoretical torsional stiffness of a circular cross-section. The Young's modulus is selected based on the initial stiffness determined from the initial slope in the experimental test curve. LS-OPT is used to compare test and simulation data. In Fig. 9 one can see comparison between the physical and the simulated tensile test together with the finite element model for this load case.

In the second step, the solid material model ****MAT_CRUSHABLE_FOAM*** is calibrated using a LS-OPT workflow for optimization and result visualization (see Fig. 11 left). The design space is reduced to six parameters defining the stress–strain curve, and a feedforward neural network serves as the metamodel with 20 design points per iteration to ensure accuracy during domain reduction (SRSM). Curve mapping, which minimizes the area between simulated and experimental curves, is used as the error metric, and two force–displacement curves from radial compression tests with a 50 mm radius indenter serve as targets for multi-objective error minimization. A satisfying optimum was as seen in Fig. 11 on the right. The comparison between tests and simulation for the optimized parameter set is visible in Fig. 12.

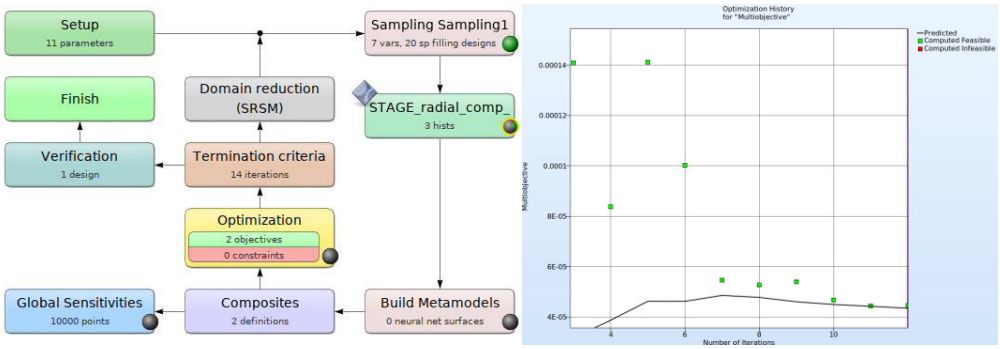

Fig. 11: Optimization workflow in LS-OPT (left) and evolution of multi-objective error during optimization (right)

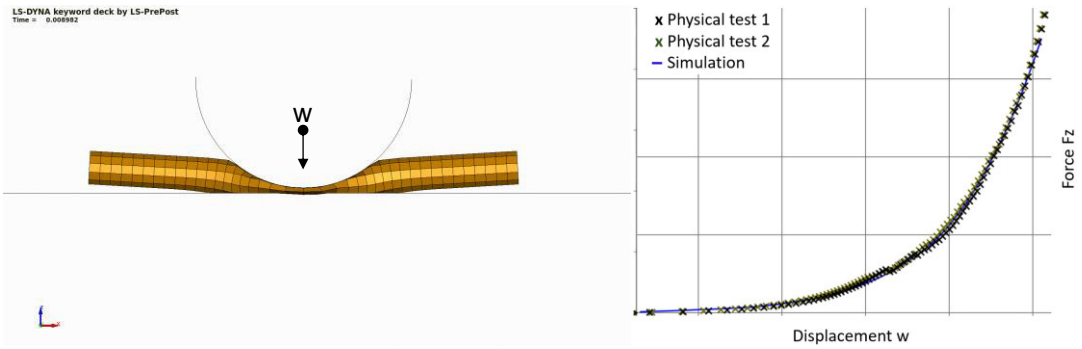

Fig. 12: Radial compression load case (R=50mm) model (left), physical and the simulated test results (right)

5.1.3 Validation

For quantitative validation, the radial compression test with a 2 mm indenter and the three-point bending test are used, while axial compression and torsion serve for qualitative assessment. LS-OPT is used to compare experimental and simulated results, showing very good agreement for radial compression (see Fig. 13) and satisfactory performance for compression and torsion (see Fig. 15); moments in bending are slightly overestimated due to retained beam stiffness but stay in an acceptable range (see Fig. 14).

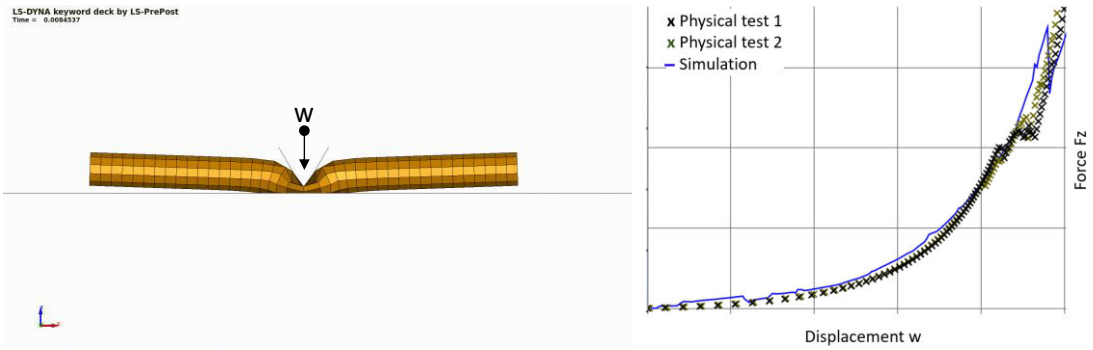

Fig. 13: Radial compression load case (R=2mm) model (left) and physical (black) and the simulated (green) test results (right)

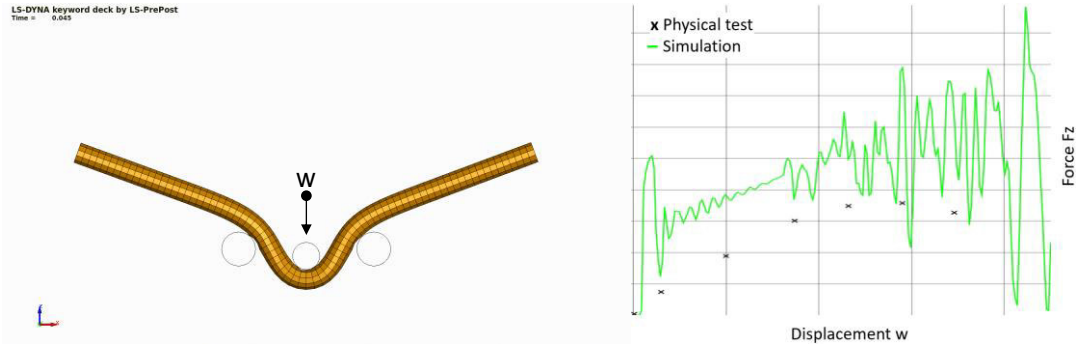

Fig. 14: Three point bending test model (left) and physical (black) and the simulated (green) test results (right)

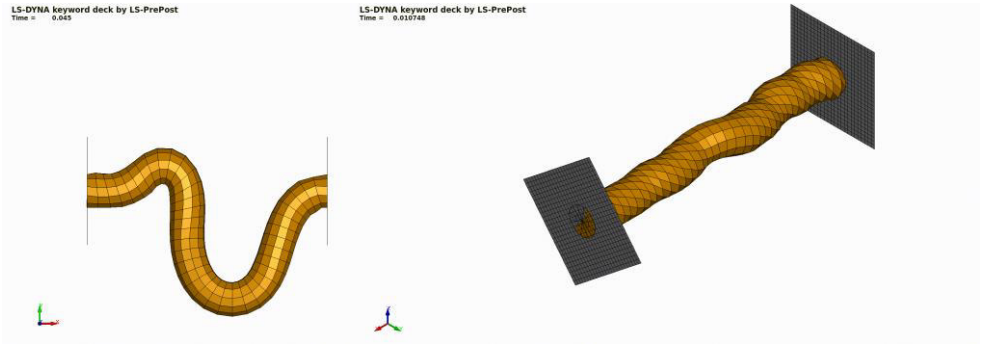

Fig. 15: Qualitative results of axial compression (left) and torsion load case (right)

6 Postprocessing

Postprocessing was conducted using LS-DYNA's **`*DATABASE_CABLE`** output, which provides time-resolved data on stress, force, and cross-sectional area for each beam element.
A custom script was developed to visualize cable stress in LS-PrePost by mapping binout results onto radial solid elements (see Fig. 16). This enabled spatial correlation between stress metrics and geometry and improves the localization of critical cable crushing scenarios, especially in full scale vehicle context.

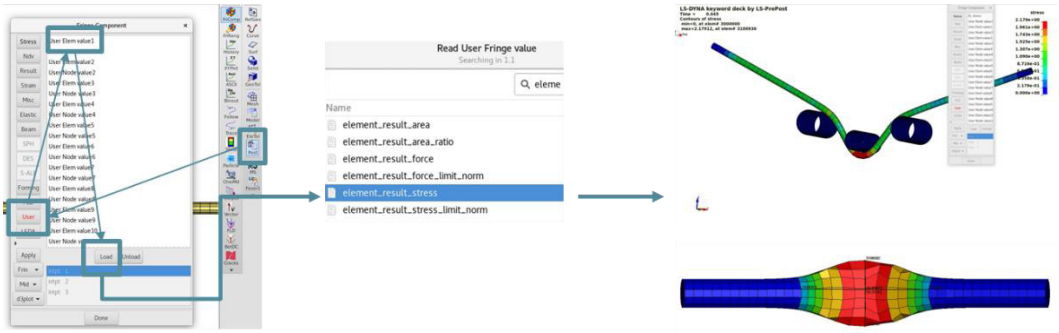

Fig. 16: User Element Result from binout to d3plot by a Python script

Short-circuit risk was assessed using maximum stress thresholds. The tool distance at short-circuit could directly be transferred from test data to simulation for identifying the according stress value at this point (see Fig. 17).

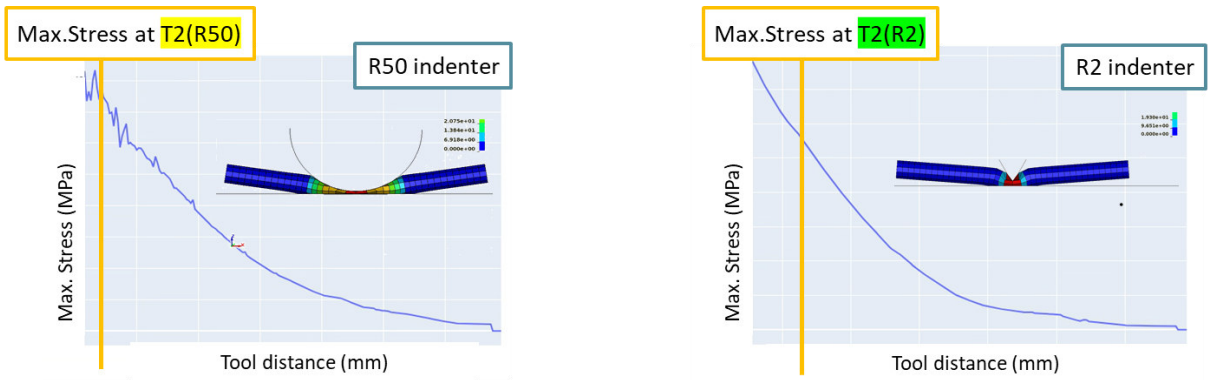

Fig. 17: Cable short-circuits Max. stress criterion related to tool distance

In a next step conservative criteria were established by considering the minimum and maximum stress values measured across a set of combinations of cable diameter and indenter type, to derive a consolidated threshold scheme for a given cable type as seen in Fig. 18. It is acknowledged that diameter- and cable-type–dependent criteria could yield higher accuracy; however, additional test data would be required to justify such an approach.

Fig. 18: Assessment scheme with conservative thresholds for one cable type

Finally, to verify the calibrated cable material, a full-scale vehicle simulation was conducted using the short-circuit thresholds as the basis for assessment. As the load case, the FMVSS 301 rear crash was selected, employing a movable and deformable barrier with an initial velocity of 80 km/h, which is expected to induce significant deformation and, consequently, cable crushing. A physical kinematic and deformation was observed, and the fringe plot reasonably highlights critical spots along the cable as demonstrated in Fig. 19.

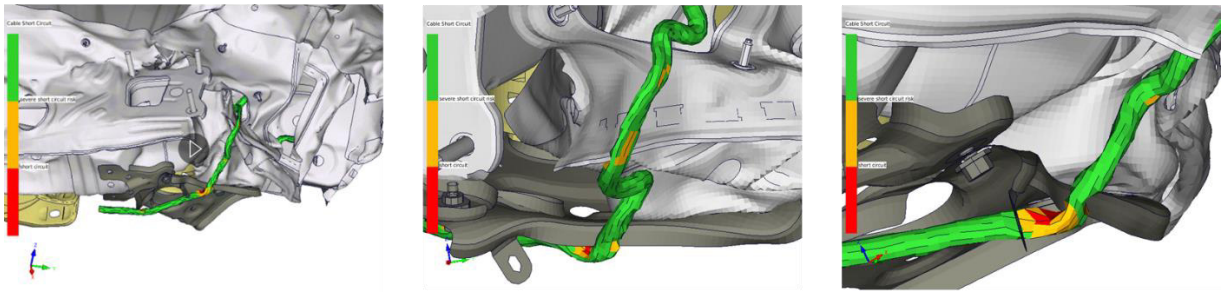

Fig. 19: Calibrated cable material and short-circuit rating applied to a full-scale vehicle simulation (load case: rear crash FMVSS 301 80 kph)

7 Summary

The calibration and validation workflow demonstrated robust capability for capturing the essential mechanical behavior of high-voltage cables under automotive crash conditions. By integrating a hybrid 1D/3D approach, the methodology successfully represents axial, bending, torsional, and transversal crushing modes, providing a realistic and computationally tractable model for HV cables in crash simulations. The ***DEFINE_CABLE** keyword proved particularly effective in enabling rapid meshing and input reduction, transforming a beam-based representation into detailed cable assemblies with minimal manual effort while preserving the critical mechanical fidelity necessary for credible predictions. The ***DATABASE_CABLE** output proved indispensable, delivering high-resolution, time-resolved information that maps cross-sectional metrics onto beam elements. This mapping allows precise localization of potential hot spots and supports informed design decisions in large-scale crash models, where understanding the spatial distribution of stress is key to improving safety and reliability.
Looking ahead, opportunities exist to extend the thresholding framework by integrating dedicated d3plot functions for cables, which would enable per-beam visualizations of maximum force, area, and maximum stress directly in the post-processing environment. ***MAT_CABLE_DISCRETE_BEAM** remains a promising candidate for broader usability due to its mesh- and diameter-independence, being based on stress-strain data; however, it currently lacks stiffness contributions for torsion and compression. Incorporating these stiffness aspects into future LS-DYNA versions would further enhance the model's versatility. Additional work could focus on expanding diameter-independent material options with consistent calibration workflows, developing diameter- and material-specific short-circuit thresholds supported by expanded test datasets, and advancing post-processing workflows to natively expose per-beam stress, force, and area metrics within standard visualization tools to reduce reliance on custom scripting.

8 Literature

[1] HEW-KABEL. HV-Systeme – Automotive. Retrieved from https://hew-kabel.com/anwendungen-loesungen/automotive/hv-systeme/, September, 2025.
[2] International Organization for Standardization. ISO 6469-3: Electrically propelled road vehicles — Safety specification — Part 3: Protection of persons against electric shock. 2021.
[3] Ansys Inc. ANSYS LS-DYNA® Keyword User's Manual, Volume I. March, 2025.